appear to be an ideal resource for transplantation therapy, and the efficacy of hiPS-NSC transplantation in SCI treatment has just begun to be investigated using the mouse model of SCI [9].

We used a recently developed protocol for the generation of long-term self-renewing neuroepithelial-like stem (lt-NES) cells, which satisfy the criteria to be defined as NSCs, from several different lines of hESCs and hiPSCs [10, 11]. hiPSC-derived lt-NES (hiPS-lt-NES) cells exhibit consistent characteristics such as continuous expandability, stable neuronal and glial differentiation ability, and the capacity to generate functional mature neurons in monolayer culture. Whereas neurosphere cultures display heterogeneous character and are sensitive to variation in methodological procedures [12], monolayer cultures offer a more homogeneous and robust cell generation [13, 14].

We report here that transplanted hiPS-lt-NES cells, derived from our robust and stable monolayer cultures, have a therapeutic potential comparable to that of NSCs from human fetal spinal cord (hsp-NSCs) for SCI in the nonobese diabetic-severe combined immunodeficient (NOD-SCID) mouse model. We further show that hiPS-lt-NES cell transplantation promotes recovery of hind limb motor function through the reconstruction of the corticospinal tract (CST), and restores disrupted neuronal circuitry in a relay manner as we have previously demonstrated in a study of mouse NSC transplantation [15]. Our results suggest that hiPS-lt-NES cells represent a promising cell source for transplantation into the injured spinal cord.

Materials and Methods

Cell Culture

hsp-NSCs and hiPS-lt-NES cells were established and maintained as described previously [10, 11, 16]. The hsp-NS cell line CB660sp and hiPS-lt-NES cell line AF22 were used in the present study. hsp-NSCs were plated onto 10 μg/ml laminin (Sigma, St. Louis, MO, http://www.sigmaaldrich.com)-coated plates in maintenance medium, consisting of Euromed-N medium (Euroclone, Milano, Italy, http://www.euroclonegroup.it), 2 mM L-glutamine, 0.1 mg/ml penicillin/streptomycin (Sigma), N2 supplement (1:100), 20 ml/l B27 (all from Invitrogen, Carlsbad, CA, http://www.invitrogen.com), 10 ng/ml fibroblast growth factor (FGF, R&D Systems, Minneapolis, MN, http://www.rndsystems.com)-2, and 10 ng/ml epidermal growth factor (EGF, R&D Systems). Cells were passaged at a ratio of 1:2 every second to third day using Accutase (Sigma). hiPS-lt-NES cells were plated onto 0.1 mg/ml poly-L-ornithine and 10 μg/ml laminin (O/L, Sigma)-coated plates in maintenance medium, consisting of Dulbecco's modified Eagle's medium/F12 (Invitrogen), 2 mM L-glutamine, 1.6 mg/ml glucose, 0.1 mg/ml penicillin/streptomycin, N2 supplement (1:100), 1 μl/ml B27, 10 ng/ml FGF2 and 10 ng/ml EGF. Cells were passaged at a ratio of 1:3 every second to third day using trypsin. To induce in vitro differentiation, hiPS-lt-NES cells were plated onto an O/L-coated 35-mm dish at a density of 5×10^5 cells per dish in culture medium without both EGF and FGF, containing 1% fetal bovine serum (FBS), and cultured for 4 weeks. Half of the medium was changed every 2 days and laminin (1:500) was added to the medium once a week to prevent detachment of the cells.

Lentivirus Production and Infection of hsp-NSCs and hiPS-Lt-NES Cells

Lentivirus production and infection of cells were performed as described previously [17, 18]. hsp-NSCs and hiPS-lt-NES cells were infected with lentiviruses harboring the luciferase and green fluorescent protein (GFP) genes connected by an internal ribosomal entry site (IRES), EFp (elongation factor promoter)-luciferase-IRES-GFP (Fig. 1B). hsp-NSCs and hiPS-lt-NES cells that had undergone more than 20 passages were infected. GFP-positive cells were collected by fluorescence activated cell sorting (FACS)-Aria II CellSorter (B.D. Biosciences, San Jose, CA, http://www.bdbiosciences.com) and used for transplantation.

SCI Model and Cell Transplantation

All aspects of animal care and treatment were carried out according to the guidelines of the experimental animal care committee of Nara Institute of Science and Technology. We used female NOD-SCID mice (8-10 weeks old, weighing 18-20 g, Charles River, Osaka, Japan, http://www.crj.co.jp). Anesthetized (ketamine 50 mg/kg, xylazine 5 mg/kg, and sodium pentobarbital 20 mg/kg) mice received laminectomies and partial laminectomies at the ninth and 10th thoracic spinal vertebrae, respectively. The dorsal surface of the dura mater was exposed and SCI was induced using an SCI device (70 kdyn; Infinite Horizon impactor, Precision Systems & Instrumentation, Lexington, KY, http://www.presysin.com) as previously described [15]. The muscle and skin were closed in layers. All mice subcutaneously received gentamicin (8 mg/kg) daily. The mice underwent manual bladder evacuation once a day. Seven days after injury, mice were anesthetized and transplanted with hiPS-lt-NES cells or hsp-NSCs using a glass micropipette attached to a stereotaxic injector (Narishige, Tokyo, Japan, http://www.narishige.co.jp). The tip of the micropipette was inserted into the injury epicenter in the injured spinal cord, and 2 μl of culture medium lacking growth factors, with or without NSCs (5×10^5 μl^{-1}), was injected at a rate of 1 μl/min.

Behavioral Testing and Electrophysiological Recordings

We evaluated the motor function of the hind limbs for up to 10 weeks after injury. Two individuals, blinded to the treatment of the mice, examined motor function using the Basso Mouse Scale (BMS) locomotor rating scale [19]. Hind limb movements of the mice were captured using a high-definition digital camcorder. We edited these movies and exported movie files using editing software.

To examine signal conduction in motor pathways after SCI, motor-evoked potentials (MEPs) at 12 weeks after SCI were measured. Mice were anesthetized with intraperitoneally injected ketamine (100 mg/kg) and their heads were fixed in a stereotactic frame. The skulls were tightly fixed to a stereotaxic apparatus (Narishige). Scalping and two small craniotomies were performed with a drill over the motor cortex area (Nakanishi, Tochigi, Japan; http://www.nsk-nakanishi.co.jp). Silver ball electrodes were placed epidurally via the holes, into which mineral oil was applied. The motor cortex was stimulated with 0.2-msecond square wave pulses at a constant current of 10 mA using an electrical stimulator (SEM-3301, Nihon Kohden, Tokyo, Japan; http://www.nihonkohden.co.jp). Recording needle electrodes were inserted into the hamstring. A subcutaneous ground electrode was placed in the tail. Electrophysiological recordings were made (MED64, Alpha MED Scientific, Osaka, Japan; http://www.amedsci.com) and band-pass filtered at 1-10 kHz. Amplitudes from onset to peak of the negative deflection were measured. Latency of MEP was measured as the time interval between the end of stimulation and the onset of the first wave. Indicated values are the average of five experiments from each mouse.

Antibodies

The following antibodies were used: rabbit anti-Sox2 (1:1,000, Chemicon-Millipore, Billerica, MA, http://www.millipore.com), mouse anti-Nestin (1:250, Chemicon), rabbit anti-brain lipid-binding protein (BLBP, 1:500, Abcam, Cambridge, U.K., http://www.abcam.com), mouse anti-β-tubulin isotype III (Tuj1; 1:500,

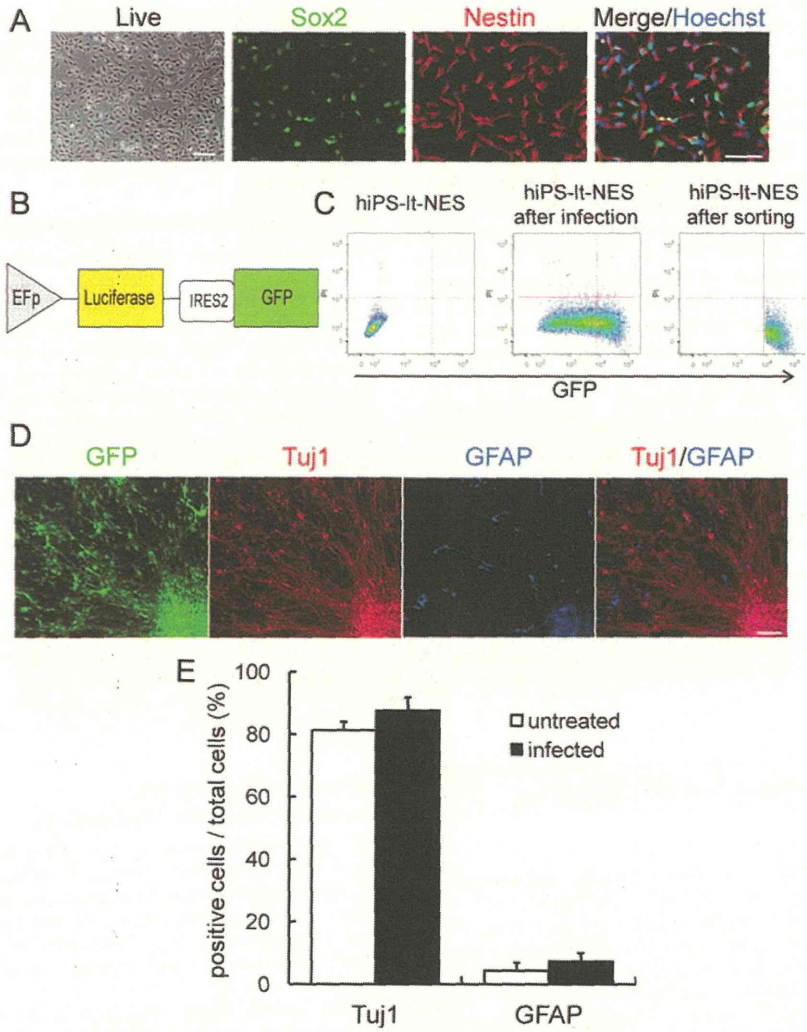

Figure 1. Characterization of hiPS-lt-NES cells. **(A):** Expansion culture. hiPS-lt-NES cells can be expanded continuously in the presence of both epidermal growth factor and fibroblast growth factor. hiPS-lt-NES cells were uniformly immunopositive for Sox2 (green) and Nestin (red). Hoechst (blue) shows nuclear staining. **(B):** The pCSII-EFp-luciferase-IRES2-GFP construct. **(C):** Flow cytometric analysis of GFP-positive cells in hiPS-lt-NES cells. Uninfected cells (left) and cells infected with lentiviruses expressing luciferase and GFP (middle) were subjected to flow cytometric analysis. GFP-positive cells in the infected cell population were sorted on the basis of GFP fluorescence and reanalyzed for GFP expression (right). **(D):** After 4 weeks in differentiation conditions, infected hiPS-lt-NES cells differentiated into Tuj1-positive neurons (red) and GFAP-positive astrocytes (blue). **(E):** Quantification of neural marker-positive cells after 4 weeks' differentiation. Lentiviral infection did not influence the differentiation tendency. Data are means ± SD ($n = 3$). Scale bars = 100 μm. Abbreviations: EFp, elongation factor promoter; GFP, green fluorescent protein; GFAP, glial fibrillary acidic protein; hiPS-lt-NES, human induced pluripotent stem cell-derived long-term self-renewing neuroepithelial-like stem; and IRES2, internal ribosomal entry site 2.

Sigma), rabbit anti-β-tubulin isotype III (Tuj1; 1:1,000, Covance, Madison, WI, http://www.covance.com), rabbit anti-GFP (1:1,000, Molecular Probes, Carlsbad, CA, http://probes.invitrogen.com), chick anti-GFP (1:500, Aves Labs, Tigard, OR, http://www.aveslab.com), rabbit anti-glial fibrillary acidic protein (GFAP, 1:2,000, DAKO, Carpinteria, CA, http://www.dako.com), mouse anti-human-specific GFAP (hGFAP, 1:1,000, STEM123, StemCells Science, Newark, CA, http://www.stemcellsinc.com), mouse anti-MAP2ab (1:500, Sigma), chick anti-myelin basic protein (MBP) (1:200, Aves Labs), mouse anti-adenomatous polyposis coli CC-1 (APC, 1:200, Calbiochem-Merck, Darmstadt, Germany, http://www.merckgroup.com), mouse anti-synaptophysin (1:200, Chemicon), mouse anti-Bassoon (Bsn, 1:400, Stressgen-Enzo Life Sciences, Plymouth Meeting, PA, http://www.enzolifesciences.com), mouse anti-human-specific synaptophysin (hSyn, 1:200, Chemicon), and mouse anti-NeuN (1:500, Millipore).

Immunocytochemistry

Immunocytochemistry experiments were performed as described previously [20]. Cells were washed with phosphate buffered saline (PBS) and fixed with 4% paraformaldehyde (PFA) in PBS for 10 minutes, and then washed with PBS and incubated in blocking solution (PBS containing 10% FBS and 0.1% Triton X-100). Subsequently, cells were incubated overnight at 4°C with the primary antibodies described above. After three washes in PBS, cells were incubated for 1 hour with the following secondary antibodies: FITC-conjugated donkey anti-chick/rabbit, Cy3-

conjugated donkey anti-chick/mouse/rabbit, Cy5-conjugated donkey anti-mouse/rabbit (1:500, Jackson ImmunoResearch, West Grove, PA, http://www.jacksonimmuno.com). After three washes with PBS, nuclei were stained with Hoechst (bisbenzimide H33258 fluorochrome trihydrochloride, Calbiochem-Merck). Samples were washed with PBS and mounted on glass slides with Immu-Mount (Thermo Scientific, Waltham, MA, http://www.thermoscientific.com). The cells were examined using a fluorescence microscope (Axiovert 200M, Zeiss, Jena, Germany, http://www.zeiss.com) equipped with the appropriate epifluorescence filters.

Immunohistochemistry

Animals were anesthetized and perfused with PBS followed by 4% PFA in 0.1 M PBS, pH 7.4. The spinal cords were dissected and postfixed overnight in the same fixative at 4°C. For cryosectioning, fixed tissues were cryoprotected in 10% sucrose in PBS overnight at 4°C, then in 20% sucrose in PBS overnight at 4°C, and embedded in optimal cutting temperature (OCT) compound (Tissue Tek, Sakura Finetek, Tokyo, Japan, http://www.sakura-finetek.com). Cryostat sections (20 μm) were cut and affixed to matsunami adhesive slide (MAS)-coated glass slides (Matsunami Glass, Osaka, Japan, http://www.matsunami-glass.co.jp). The sections were permeabilized in PBS-T (PBS containing 0.1% Triton X-100) for 10 minutes and blocked with 10% FBS in PBS-T for 1 hour, and then incubated overnight at 4°C with the primary antibodies described above. After three washes with PBS, they were incubated in a mixture of the secondary antibodies described above for 1 hour. After a final rinse with PBS, nuclei were stained using Hoechst. Sections were mounted and examined under a fluorescence microscope (Axiovert 200M, Zeiss) and a scanning laser confocal imaging system (LSM 710, Zeiss).

In Vivo Imaging of Transplanted Cells

In vivo imaging experiments were performed as described previously [18]. A Xenogen-IVIS 100 cooled CCD optical macroscopic imaging system (SC BioScience, Tokyo, Japan, www.scbio.co.jp) was used for bioluminescence imaging. Mice were given an intraperitoneal injection of D-luciferin (150 mg/kg) and serial images were acquired from 20 minutes after administration until the maximum intensity was obtained with the field-of-view set at 10 cm. All images were analyzed using Igor (WaveMetrics, Portland, OR, http://www.wavemetrics.com) and Xenogen Living Image software, and optical signal intensity was expressed as photon flux in units of photons/s per cm^2/steradian. To quantify the measured light, we defined regions of interest (ROIs) over the cell-implanted area and examined all values within the same ROI. The obtained photon count intensity was expressed as a percentage of the initial value.

Anterograde Labeling of the CST

Twelve weeks after injury, descending CST fibers were labeled with biotinylated dextran amine (BDA) (MW 10,000, 10% in saline, 2 μl per cortex; Molecular Probes) [21, 22] by injection into the left and right motor cortices [23]. The skulls of anesthetized mice were tightly fixed to a stereotaxic apparatus (Narishige). Scalping and craniotomy over the motor cortex area were carried out using a micromotor system (Nakanishi). The injection site was 2.1 mm posterior to the bregma, 2 mm lateral to the bregma, and 0.7 mm in depth [23]. For pressure injections with a 20-μm outer diameter glass capillary attached to a microsyringe (Narishige), we used 0.1-μl steps per minute until the desired volume (1 μl per injection site) was injected. Two weeks later, the animals were perfused and their spinal cords were fixed as described above. Sections (30 μm) were cut and used for immunohistochemistry. To visualize the BDA, a tyramide signal amplification fluorescence system (Perkin Elmer, Waltham, MA, http://www.perkinelmer.com) was used.

Visualization of Multisynaptic Neural Pathways

To visualize selective and functional transsynaptic neural pathways, wheat germ agglutinin (WGA)-expressing recombinant adenoviruses were used [24, 25]. Twelve weeks after injury, 1 μl of saline containing WGA-expressing virus at a titer of 1×10^{11} pfu/ml was injected into the bilateral motor cortices (0.5 μl per injection site). The injection site was 2.1 mm posterior to the bregma, 2 mm lateral to the bregma, and 0.7 mm in depth. Two weeks later, animals were perfused and the spinal cords were fixed as described above. Sections (15 μm) were cut and used for immunohistochemistry. Rabbit anti-WGA polyclonal antibody (3 μg/ml, Sigma) was preabsorbed with 1% acetone powder of mouse brains in blocking solution overnight at 4°C.

Ablation of Transplant-Derived Cells

Cell ablation experiments were performed as described previously [26, 27]. Diphtheria toxin (DT) was purified from conditioned medium of the PW8 strain of *Corynebacterium diphtheriae* by diethylaminoethyl Sepharose column chromatography and diluted to an appropriate concentration with saline. Seven weeks after injury, DT solution (50 μg/kg per day $\times$ 2 days) was administered by intraperitoneal injection into seven hiPS-NES cell-transplanted mice.

Statistical Analysis

We performed statistical analysis with an unpaired two-tailed Student's t test for single comparisons. For &&&BMS and BDA fiber analysis, we used repeated-measures analysis of variance (ANOVA) with Tukey-Kramer multiple comparison test at each point (Prism, GraphPad, LA Jolla, CA, http://www.graphpad.com). $p < .05$ was considered significant.

Results

Characterization of hiPS-Lt-NES Cells In Vitro

We have previously shown that hiPS-NES cells, which are reliably derived from different hiPS cell lines, exhibit consistent characteristics such as continuous expandability, stable neuronal and glial differentiation, and the capacity to generate functional mature human neurons [11]. hiPS-lt-NES cells can be expanded in the presence of FGF2 and EGF in monolayer culture, and express the NSC markers Sox2 and Nestin (Fig. 1A) and the radial glial marker BLBP (Supporting Information Fig. 1), but not the ES/iPS cell markers Oct3/4 or Nanog (not shown).

To visualize transplanted cells by both luminescence and fluorescence, hiPS-lt-NES cells were infected with lentiviruses engineered to express luciferase and GFP (Fig. 1B). Almost all hiPS-lt-NES cells were infected (Fig. 1C, middle), and we isolated only strongly GFP-expressing cells for use in subsequent in vitro and transplantation experiments (Fig. 1C, right).

We then examined whether lentiviral infection affected the differentiation potential of hiPS-lt-NES cells. Uninfected and infected hiPS-lt-NES cells were induced to differentiate by removal of growth factors and cultured in the presence of 1% FBS for 4 weeks. Both hiPS-lt-NES cell population differentiated into large and small numbers of Tuj1-positive neurons and GFAP-positive astrocytes, respectively, as observed in our previous study [11] (Fig. 1D). Quantitative analysis revealed no significant differences in the proportions of differentiated cells between uninfected and infected hiPS-lt-NES cells (Fig. 1E). Thus, we concluded that lentiviral infection did not influence the differentiation potential of hiPS-NES cells.

Transplantation of hiPS-Lt-NES Cells into the Injured Spinal Cord Improves Functional Recovery of Hind Limbs

In the present study, we used NOD-SCID mice, which are a suitable model for xenograft research because they are constitutively immunodeficient; their pathology and innate immune response after SCI are also similar to those of other mouse strains [4, 9, 28].

Previous studies have already shown that transplantation of human NSCs from fetal spinal cord or brain tissue improves locomotor functional recovery of SCI models [3, 4]. Nevertheless, only recently has the efficacy of hiPS-NSC transplantation into SCI begun to be investigated [9]. To determine whether our hiPS-lt-NES cells have a therapeutic capability, we first sought to compare the effects of these cells with those of human fetal spinal cord-derived NSCs (hsp-NSCs). Seventy-kilodyne contusive SCI was applied at the ninth thoracic vertebral level of mouse spinal cords, and 1 week later we injected medium alone (SCI control), or medium containing hsp-NSCs or hiPS-lt-NES cells, into the epicenter. We then monitored the animals' hind limb motor function using the BMS [19] for at least 8 weeks. All mice showed complete paralysis at 1-day after SCI (BMS scores were 0, Supporting Information Video 1). At 8 weeks after SCI, control mice could move their hind limbs but could not support their own weight (BMS scores were approximately 2, Supporting Information Video 2). In contrast, mice that received hsp-NSCs could touch the ground with their paws and/or support their body weight using their hind limbs (BMS scores were 3-4). The hiPS-lt-NES cell-transplanted group also showed functional recovery (BMS scores were 3-4, Supporting Information Video 3) compared to the control group, and there was no significant difference in BMS scores between the hsp-NSC- and hiPS-lt-NES cell-transplanted groups (Fig. 2A). These results indicate that hiPS-NES cells have a comparable therapeutic effect to hsp-NSCs on SCI.

Next, to evaluate the recovery of descending pathways from the motor cortex to the hind limb motor neurons, we monitored MEPs at 12 weeks after SCI. We stimulated motor cortices electrically and recorded MEP amplitudes from the hamstring muscles. The MEP amplitudes in the hiPS-NES cell-transplanted group were significantly higher than those in the SCI control group (Fig. 2B, 2C). Furthermore, the latency of MEP response in the hiPS-lt-NES cell-transplanted group was significantly shorter than that in the SCI control group (Fig. 2D). These results suggest that transplantation of hiPS-lt-NES cells into the injured spinal cord stimulates the functional recovery of hind limbs.

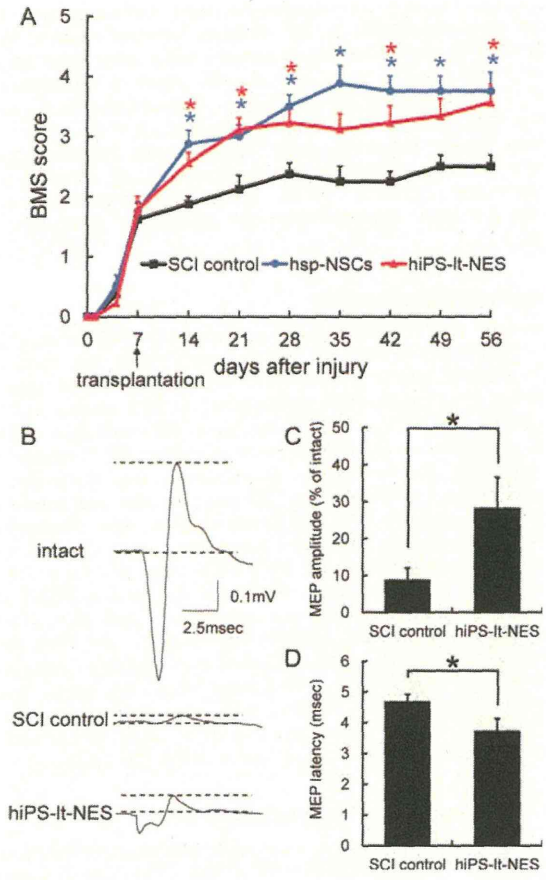

Figure 2. Transplantation of hiPS-lt-NES cells into the injured spinal cord improves functional recovery of hind limbs. **(A):** Time course of functional recovery of hind limbs after SCI. Data are means ± SEM (SCI control, $n = 8$; hsp-NSCs, $n = 8$; hiPS-lt-NES cells, $n = 9$). Mean BMS values of hsp-NSC- and hiPS-lt-NES cell-transplanted groups were compared with those of the SCI control group. *, $p < .05$. There was no significant difference between values in the hsp-NSC group and the hiPS-lt-NES cell group. **(B):** Representative MEP waves of intact, SCI control, and hiPS-lt-NES cell-treated mice at 12 weeks after injury. The motor cortices were stimulated and MEP amplitudes were recorded from hamstring muscles. Amplitudes from onset to peak of the negative deflection were measured. **(C):** Relative values of the mean MEP amplitudes. Values are expressed as percentages of those in intact mice. Mean relative MEP amplitude in the hiPS-lt-NES cell group was significantly higher than that in the SCI control group. *, $p < .05$. Data are means ± SD ($n = 3$). **(D):** Relative values of the mean MEP latency. Mean relative MEP latency in the hiPS-lt-NES cell group was significantly shorter than that in the SCI control group. *, $p < .05$. Data are means ± SD ($n = 3$). Abbreviations: BMS, Basso Mouse Scale; hiPS-lt-NES, human induced pluripotent stem cell-derived long-term self-renewing neuroepithelial-like stem; MEP, motor-evoked potential; hsp-NSC, human fetal spinal cord-derived neural stem cell; and SCI, spinal cord injury.

Transplanted hiPS-Lt-NES Cells Survive and Differentiate in the Injured Spinal Cord of NOD-SCID Mice

We have established hiPS-lt-NES cells that express luciferase and GFP, enabling us to trace the survival of the transplanted cells with a bioluminescence imaging system which detects photon signals from living cells after administration of luciferin (a substrate of luciferase) to the mice [18]. The photon signals decreased gradually after transplantation (Fig. 3A) and approximately 20% of transplanted hiPS-lt-NES cells survived in the injured spinal cord at 5 weeks after SCI (4 weeks after transplantation), whereafter the photon signals remained stable (Fig. 3B).

Using immunohistochemistry, we found that GFP-positive transplanted cells survived and migrated to both rostral and caudal areas around the lesion site in the injured spinal cord (Fig. 3C). High-magnification images showed that transplanted hiPS-lt-NES cells extended processes into both gray and white matter (Fig. 3C-1, 3C-2).

We then examined the differentiation of the transplanted hiPS-lt-NES cells in the injured spinal cord and found a similar differentiation tendency to that observed in vitro (Fig. 1D, 1E), with many GFP-positive transplant-derived cells having become Tuj1-positive neurons (75%) at 8 weeks after SCI (Fig. 3D–3F). Twenty percent of GFP-positive transplanted cells differentiated into GFAP-positive astrocytes, while their

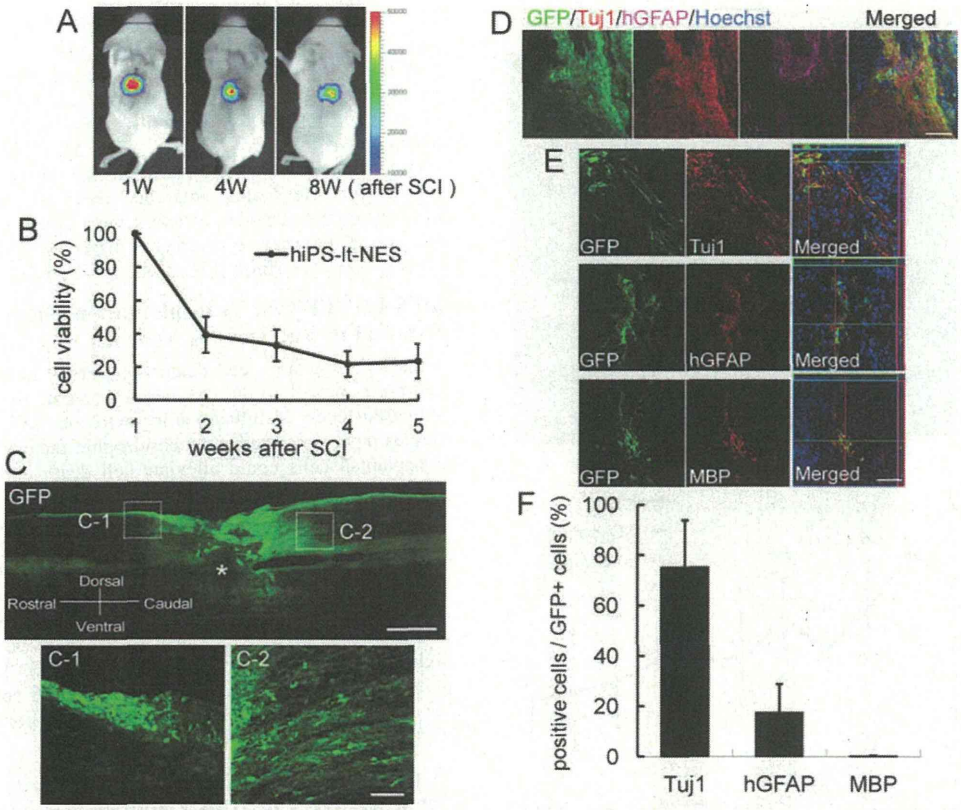

Figure 3. Transplanted human induced pluripotent stem cell-derived long-term self-renewing neuroepithelial-like stem (hiPS-lt-NES) cells survive and differentiate in the injured spinal cord of nonobese diabetic-severe combined immunodeficient mice. **(A):** Survival of transplanted cells was checked every week using a bioluminescence imaging system; left, 2 hours after transplantation; middle, 4 weeks after SCI; and right, 8 weeks after SCI. **(B):** Time course of transplanted hiPS-lt-NES cell survival in SCI model mice. Optical signal intensity was measured using the bioluminescence imaging system. Quantification of the photon intensity revealed that approximately 20% of the transplanted cells survived 5 weeks after SCI; thereafter, the photon signals remained stable. Data are means ± SEM ($n = 6$). **(C):** Sagittal sections of SCI model mice treated with hiPS-lt-NES cells at 8 weeks after transplantation. Sections were stained with anti-GFP antibody (green). The epicenter of the SCI is indicated (*). Higher-magnification images of the white dotted boxes (C-1 and C-2) show GFP-positive transplant-derived cells extending their processes into gray and white matter. **(D):** Immunostaining images, 8 weeks after injury, of hiPS-lt-NES cells grafted into spinal cord. Spinal cord sections were stained with anti-GFP (green), hGFAP (magenta) and Tuj1 (red) antibodies and with Hoechst (blue). **(E):** Confocal images, 8 weeks after injury, of hiPS-lt-NES cells transplanted into spinal cord, revealing transplanted cells which were double-positive for GFP and markers of neural lineages. **(F):** Quantitative analyses of Tuj1-positive neurons, hGFAP-positive astrocytes, and MBP-positive oligodendrocytes as in E. Data are means ± SD ($n = 3$). Scale bars = 500 μm in C, 100 μm in C-1, C-2, D, and E. Abbreviations: GFP, green fluorescent protein; hGFAP, anti-human-specific glial fibrillary acidic protein; MBP, and SCI, spinal cord injury.

differentiation into MBP- or APC-positive oligodendrocytes was less than 1% (Fig. 3E, 3F, Supporting Information Fig. 2). These data indicate that transplanted hiPS-lt-NES cells differentiate preferentially into neurons in the injured spinal cord.

hiPS-Lt-NES Cell Transplantation Does Not Promote CST Axon Re-Extension After SCI

Since transplanted NSCs have been reported to play a supportive role in the re-extension of injured axons [29], we examined the effect of the transplanted hiPS-lt-NES cells on CST first-order axonal regeneration. We injected BDA into the bilateral motor cortices and labeled CST first-order neuron axons by anterograde tracing [21, 22]. Because BDA is not transported from first- to second-order neurons across the synapse, only the axons of first-order neurons in the CST are visualized by this method.

In the region caudal to the injury site, >50% of the labeled fibers observed at 5 mm anterior to the lesion site were detected in the intact mice, whereas almost no BDA-traced CST fibers could be seen in the SCI control or hiPS-lt-NES cell-transplanted mice (Fig. 4A). Quantitative analysis revealed that there was no significant difference in the number of BDA-labeled fibers between the SCI control and hiPS-lt-NES cell-treated groups at any position up to 5 mm on either side of the lesion site (Fig. 4B). Although we cannot exclude possibilities such as the re-extension of descending raphespinal axons, which are also important for the motor functional recovery of hind limbs [30, 31], these results suggest that the regeneration of CST axons, if it occurs, cannot be a major contributing factor in the recovery induced by hiPS-lt-NES cell transplantation in our SCI model.

Local Neurons Reconstruct Disrupted CST Neuronal Circuits in a Relay Manner

Recent studies have revealed that local endogenous and transplant-derived neurons can form new neuronal circuits and make synaptic connections after SCI [32–34]. To determine

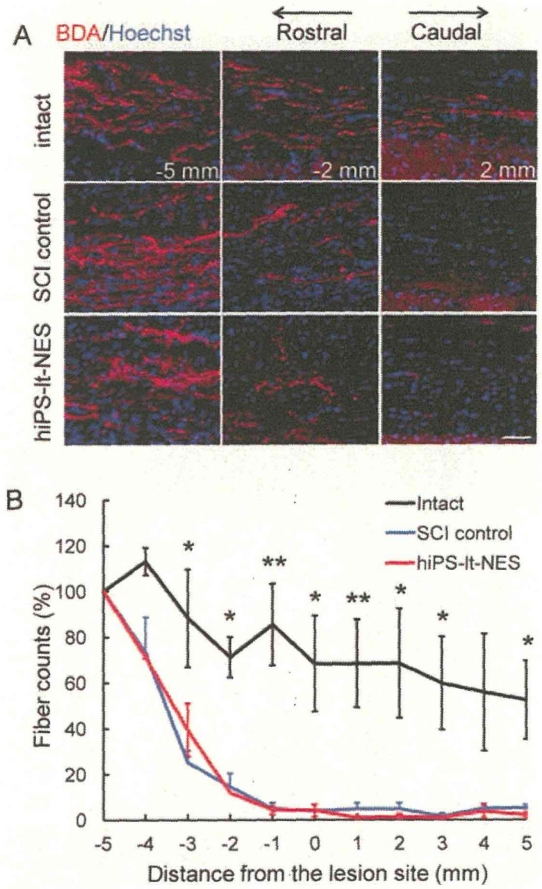

Figure 4. hiPS-lt-NES cell transplantation does not promote corticospinal tract (CST) axon re-extension after SCI. **(A):** Representative pictures of BDA-labeled CST fibers (red) at 5 and 2 mm rostral and 2 mm caudal to the lesion site at 12 weeks after SCI. Hoechst (blue) shows nuclear staining. Scale bar = 50 μm. **(B):** Quantification of the labeled CST fibers in the spinal cords of untreated, SCI control, and hiPS-lt-NES cell-transplanted mice. The x-axis indicates specific locations along the rostro-caudal axis of the spinal cord, and the y-axis indicates the ratio of the mean number of BDA-labeled fibers at the indicated site to that at 5 mm rostral to the lesion site (thoracic vertebra [Th] 9). Intact mice were compared with SCI control mice. *, $p < .05$; **, $p < .01$. There was no significant difference in the number of BDA-labeled fibers between hiPS-lt-NES cell-treated (blue line) and SCI control groups (red line). Data are means ± SEM ($n = 5$). Abbreviations: BDA, biotinylated dextran amine; hiPS-lt-NES, human induced pluripotent stem cell-derived long-term self-renewing neuroepithelial-like stem; and SCI, spinal cord injury.

whether disrupted CSTs were reconstructed by forming a local neuronal relay, we injected WGA-expressing adenoviruses into the motor cortex of the hind limb area at 12 weeks after SCI. WGA, a plant lectin, has been widely used as a tracer of neuronal pathways [24, 25] because it is transported in axons and dendrites, and across synapses, to second- and even third-order neurons.

After injection, we could detect WGA-immunoreactive intracellular granule-like structures in MAP2ab-positive neurons (Fig. 5A). Furthermore, we found that hiPS-lt-NES cell-treated mice had more WGA/Map2ab double-positive cells than SCI control mice in the caudal region below the injured site (Fig. 5A, 5B). Taking these data and the results of the BDA experiment into consideration, it is suggested that WGA was transferred to the caudal area through the lesion site via new synaptic connections, and that hiPS-lt-NES cell transplantation promoted the CST reconstruction without CST axonal re-extension. In support of this proposition, we could observe GFP-positive transplant-derived neurons adjacent to synaptophysin-positive patches (Fig. 5C-1 and 5C-1′). Furthermore, immunohistochemistry using species-specific antibodies for presynaptic markers revealed that transplant-derived neurons made synapses with endogenous neurons, suggesting that they reconstructed disrupted CST neuronal circuits in a relay fashion (Fig. 5C-2, 5C-2′, 5C-3, and 5C-3′).

hiPS-Lt-NES Cell Transplantation Promotes the Survival of Endogenous Neurons

Massive endogenous cell death is observed in the injured spinal cord, probably due to environmental changes such as increased levels of inflammatory cytokines [35, 36]. Previous studies have suggested that neurotrophic factors secreted from transplanted cells could alleviate cell death and thereby contribute to improved locomotor function after SCI [37]. We therefore wanted to examine whether transplanted hiPS-lt-NES cells influence the survival of endogenous neurons. We performed immunohistochemistry and counted the number of NeuN-positive/GFP-negative endogenous neurons around the lesion site (Fig. 6A) and found that the number of endogenous neurons in the hiPS-lt-NES cell-treated mice was significantly higher than that in the SCI control (Fig. 6B). These findings indicate that transplantation of hiPS-lt-NES cells alters the environment of the injured spinal cord and promotes the survival of endogenous neurons.

Transplanted Cells Contribute Directly to Functional Recovery of Hind Limb Movement in SCI Model Mice

Ablation of specific cells is a useful method to evaluate their functional contribution in animal models. Mouse and rat cells are less sensitive to DT than human cells, which express human heparin-binding epidermal growth factor-like growth factor (hHB-EGF) as a DT receptor [26, 27]. We administered DT to hiPS-lt-NES cell-transplanted mice at 7 weeks after SCI. Using an in vivo imaging system, we were able to trace the survival of transplanted cells while evaluating hind limb function. Almost all the transplanted hiPS-lt-NES cells were specifically ablated following DT administration (Fig. 7A). After ablation of the transplanted cells, the BMS score of hiPS-lt-NES cell-treated mice dropped to a level similar to that of SCI control mice, although the reduction was not large enough to make the score differ significantly from that attained by hiPS-lt-NES cell-treated mice without DT administration (Fig. 7B). This may be because transplanted hiPS-lt-NES cells promoted the survival of endogenous neurons (Fig. 6) that participated in the reconstruction of disrupted neuronal circuitry. Nevertheless, these results suggest that transplanted hiPS-lt-NES cells play direct and important roles in the functional recovery of the injured spinal cord.

Discussion

The advent of cell reprogramming and the establishment of iPS cells have provided new prospects for stem cell transplantation therapy [7, 8], and a large number of different types of iPSCs have already been generated by various methods [38–40]. Transplantation of NSCs into the injured spinal cord has been shown to be effective, and with recent advances in stem cell biology, particularly in human ES/iPS cells, we anticipate

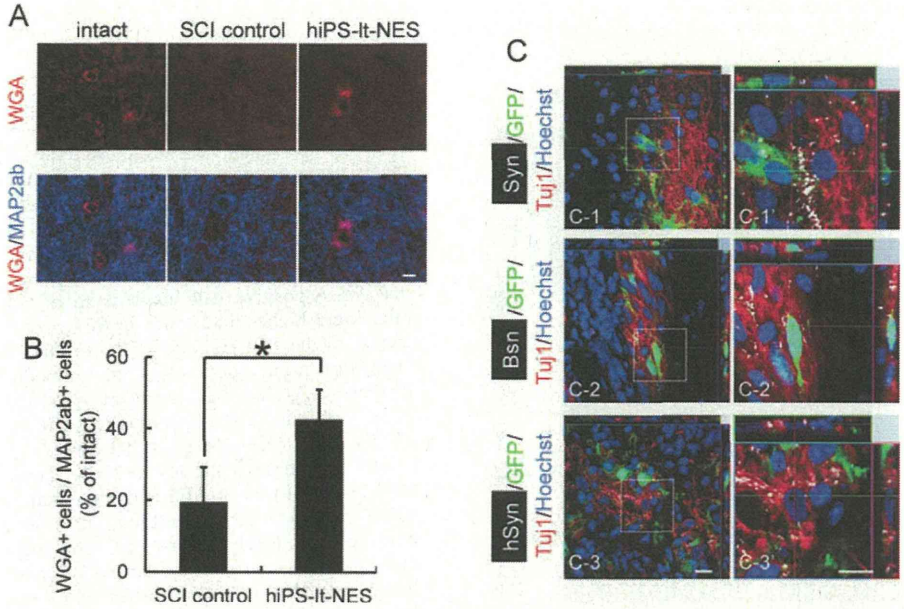

Figure 5. Local neurons reconstruct disrupted corticospinal tract neuronal circuits in a relay manner. **(A):** Representative pictures of WGA-labeled neuronal cell bodies located in the caudal area (Th11 to lumbar vertebra [L] 1) at 12 weeks after spinal cord injury (SCI; left, intact mice; middle, SCI control mice; and right, hiPS-lt-NES cell-treated mice). Spinal cord sections were stained with anti-WGA (red) and anti-MAP2ab (neuronal marker, blue) antibodies. WGA immunoreactivity was observed as intracellular granule-like structures. **(B):** WGA-positive cells/MAP2ab-positive neurons in the caudal area were quantified. Values are expressed as percentages of those in intact mice. The percentage of WGA-positive cells in hiPS-lt-NES cell-treated mice was significantly higher than that in SCI control mice. *, $p < .05$. Data are means ± SD ($n = 3$). **(C):** Spinal cord sections were stained with anti-GFP and Tuj1 antibodies, Hoechst (blue), and Syn, Bsn, or hSyn antibodies. (C-1) Representative confocal image showing that GFP (green) and Tuj1 (red) double-positive transplant-derived neurons were adjacent to synaptophysin-positive patches (white). (C-1′) High-magnification view of boxed area in (C-1). (C-2) Host and graft synapses were distinguished using a monoclonal antibody for the presynaptic marker Bsn that selectively recognizes rat and mouse, but not human, epitopes. Confocal image showing that GFP (green) and Tuj1 (red) double-positive transplant-derived neurons were in contact with Bsn-positive host synapses (white). (C-2′) High-magnification view of boxed area in (C-2). (C-3) Confocal images showing that GFP (green)-negative and Tuj1 (red)-positive endogenous neurons were in contact with hSyn-positive synapses (white). (C-3′) High-magnification view of boxed area in (C-3). Scale bars = 10 μm. Abbreviations: Bsn, anti-Bassoon; GFP, green fluorescent protein; hiPS-lt-NES, human induced pluripotent stem cell-derived long-term self-renewing neuroepithelial-like stem; hSyn, anti-human-specific synaptophysin; Syn, anti-synaptophysin; and WGA, wheat germ agglutinin.

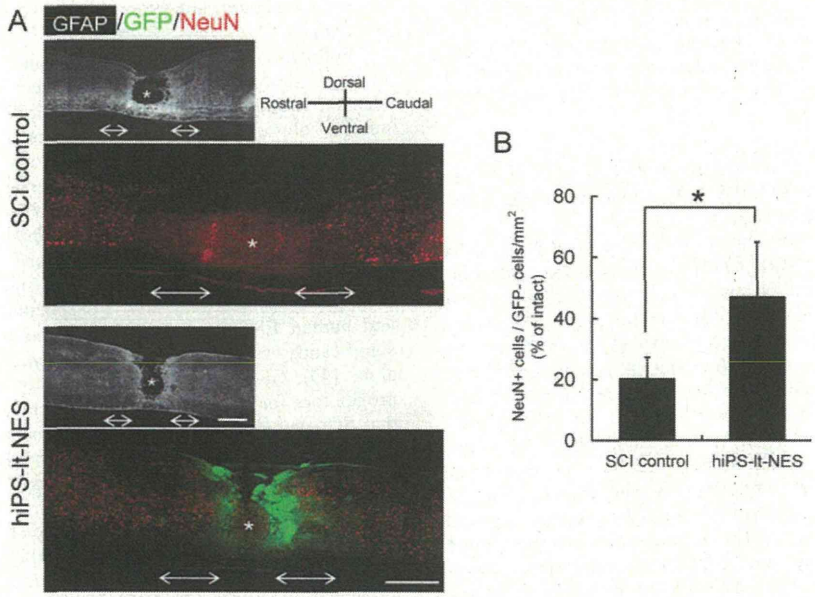

Figure 6. Transplanted hiPS-lt-NES cells promote the survival of endogenous neurons. **(A):** Representative sagittal sections of SCI control and hiPS-lt-NES cell-transplanted mice at 12 weeks after SCI. Sections were stained with anti-GFAP (white), anti-NeuN (mature neuronal marker, red) and anti-GFP (green) antibodies. Two 500-μm regions, at the rostral and caudal edge of the lesioned site (double-headed arrows), were selected for the assessment. The epicenter of the SCI is indicated (*). Scale bars = 500 μm. **(B):** Quantification of NeuN-positive/GFP-negative endogenous neurons. Values are expressed as percentages of those in intact mice. The number of NeuN-positive/GFP-negative endogenous neurons in hiPS-lt-NES-treated mice was significantly higher than that in SCI control mice. *, $p < .05$. Data are means ± SD ($n = 3$). Abbreviations: GFAP, glial fibrillary acidic protein; GFP, green fluorescent protein; hiPS-lt-NES, human induced pluripotent stem cell-derived long-term self-renewing neuroepithelial-like stem; and SCI, spinal cord injury.

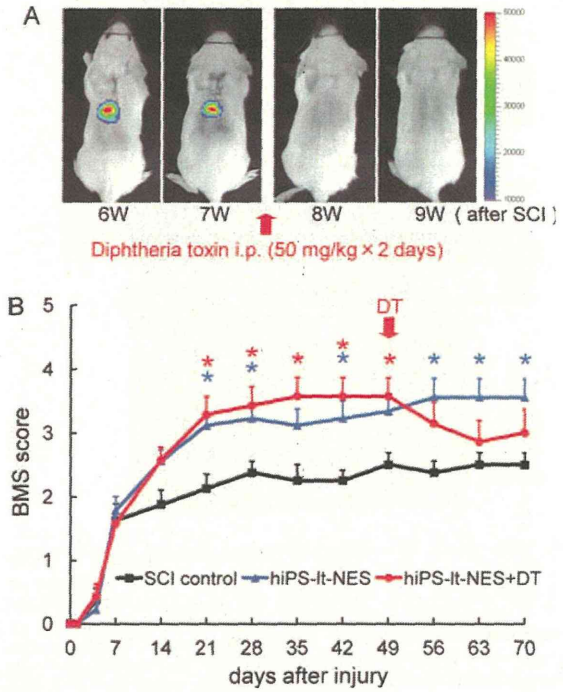

Figure 7. Transplanted cells contribute directly to the functional recovery of hind limb movement in SCI model mice. **(A):** Survival of transplanted cells was monitored using a bioluminescence imaging system. Seven weeks after SCI (6 weeks after transplantation), each mouse was administered DT. One week later, luciferase activity had completely disappeared in hiPS-lt-NES cell-transplanted mice. **(B):** Time course of functional recovery of hind limbs after SCI and DT administration. Data are means ± SEM (SCI control, $n = 8$; hiPS-lt-NES, $n = 9$; and hiPS-lt-NES+DT, $n = 7$). Hind limb function of hiPS-lt-NES cell-transplanted mice deteriorated after DT administration (red line). BMS values of the hiPS-lt-NES and hiPS-lt-NES+DT groups were compared with those of the SCI control group. *, $p < .05$. Abbreviations: BMS, Basso Mouse Scale; DT, diphtheria toxin; hiPS-lt-NES, human induced pluripotent stem cell-derived long-term self-renewing neuroepithelial-like stem; and SCI, spinal cord injury.

further improvements in the treatment of SCI [41]. However, transplantation studies of hiPS-NSCs, initially using mouse models of SCI [9], are in their infancy.

We have previously shown that human lt-NES cells, derived from different hESC and iPSC lines in two independent laboratories, exhibit consistent characteristics and retain their ability to proliferate and differentiate even after several passages and long-term in vitro growth [11]. In the present study, we investigated the differentiation potential of transplanted hiPS-lt-NES cells and found that the majority of differentiated hiPS-lt-NES cells in the injured spinal cord were neurons (Fig. 3D–3F), even though endogenous or transplanted NSCs in the injured spinal cord have been reported by others to differentiate preferentially into the glial lineage [42, 43]. Recent studies have indicated that neurons derived from transplanted human NSCs can integrate into the injured spinal cord and form synaptic connections with host neurons [33, 34]. We therefore took advantage of the tendency of our hiPS-lt-NES cells to differentiate into neurons and tried to apply these cells to reconstruction of the injured spinal cord.

Multiple therapeutic effects of NSC transplantation have been reported, and many different types of stem cells have been grafted into the injured spinal cord, yielding improved functional recovery in animal models [44, 45]. However, the growth of axons through the lesion to reinnervate the side caudal to the injury has so far been very limited. Our experiments using anterograde labeling of CST fibers revealed that this was also the case after transplantation of hiPS-lt-NES cells (Fig. 4). We have previously shown that neurons derived from mouse NSCs could restore disrupted neuronal circuits [15]. Consistent with that observation, we demonstrated here that WGA-positive cell numbers in hiPS-lt-NES cell-treated mice were higher than those in SCI control mice in the area caudal to the SCI (Fig. 5A, 5B). Furthermore, immunohistochemistry using species-specific antibodies for presynaptic markers suggested that transplant-derived neurons made synapses with endogenous neurons (Fig. 5C-2, 5C-2′, 5C-3, and 5C-3′). These results suggest that WGA was transferred to the caudal area through the lesion site via new synaptic connections, and that hiPS-lt-NES cell transplantation promoted CST reconstruction in a relay fashion. Other studies have provided evidence that local neurons can form intraspinal neural circuits in the lesion site and make synaptic connections with descending-tract collaterals after SCI [32, 46], and human NSCs transplanted into the injured rat or mouse spinal cord differentiated into neurons that formed axons and synapses, and also established contacts with host neurons [4, 34].

As well as their roles in cell replacement, NSCs reportedly exert other effects through the secretion of neurotrophic factors [37], which, by means such as suppressing myelin inhibitors, prevent neuronal cell death, enhance remyelination and regenerate axons [47, 48]. We found that transplantation of hiPS-lt-NES cells supported the survival of endogenous neurons (Fig. 6). Conversely, ablation of transplanted cells decreased previously attained functional recovery (Fig. 7), suggesting that transplanted cells contribute directly to functional recovery of hind limb movement in SCI model mice. In summary, we suggest that not only neurons derived from transplanted hiPS-lt-NES cells but also surviving endogenous neurons contribute to functional improvement by forming multiple synaptic connections which restore disrupted neuronal circuits.

Following injury, demyelinated and reconstructed axons must be remyelinated to ensure proper functional recovery. Generally, endogenous or transplanted NSCs which differentiate into oligodendrocytes have been reported to contribute to remyelination of axons and thereby to help in recovery after SCI. Transplanted oligodendrocyte progenitor cells (OPCs) derived from human ESCs have been shown to differentiate into oligodendrocytes and enhance remyelination in the moderate rat model of contusion spinal cord injury [5, 6]. A further study reported that in complete spinal cord transection rats, locomotor recovery after transplantation with both OPCs and human ESC-derived motor neuron progenitor cells was significantly greater than after treatment with either cell type alone [49]. Given that the application of stem cells and their progenitors for transplantation is currently in its infancy, and that SCI pathology differs between contusion and transection [50], these findings indicate that neural cells in an appropriate lineage should be transplanted according to the degree and/or type of SCI.

When ES and iPS cells are used for transplantation treatment, a key consideration is the likelihood of tumor formation, since the transplanted cell population may include undifferentiated cells [51, 52]. Indeed, the sources and methods of induction of NSCs are critical for differentiation and tumor formation [33, 53]. Neurosphere cultures are heterogeneous and sensitive to variations in methodological procedures [12], whereas monolayer cell cultures give rise to more homogeneous population [13, 14]. In this study, we detected no tumor

formation in more than 40 hiPS-lt-NES cell-treated mice up to 12 weeks after SCI. This is probably attributable to complete differentiation of hiPS cells into NES cells in our robust and stable monolayer cell cultures, since the NES cells were established by initially purifying neural rosette structures from differentiating cultures [11]. Furthermore, we transplanted hiPS-lt-NES cells which had been expanded in the presence of growth factors and passaged more than 20 times. Before human iPS cell-based therapies can be implemented for clinical application, the cells' proliferation and tumor formation after transplantation must be strictly evaluated.

Conclusion

In this study, we have demonstrated that hiPS-lt-NES cells survived and differentiated in the injured spinal cord of NOD-SCID mice, and promoted functional recovery of hind limbs. Moreover, we have shown that transplanted hiPS-lt-NES cells support the reconstruction of CST pathways, promote endogenous neuron survival, and directly contribute to improved hind limb movement. To achieve a more efficient treatment for SCI, detailed investigations of hiPS-lt-NES cells and SCI pathology will be necessary. Nevertheless, our study raises the possibility that hiPS-based therapy can be applied in the near future to SCI patients who currently have few or no therapeutic options.

Acknowledgments

We thank M. Saito and K. Kohno for providing diphtheria toxin, H. Miyoshi, H. J. Okano, and H. Okano for lentiviral vectors, Y. Yoshihara for WGA-expressing adenovirus, N. Uchida for anti-human specific antibodies, and S. Nori and M. Nakamura for species-specific antibodies. We also thank Y. Bessho, T. Matsui, Y. Nakahata, T. Matsuda, S. Komai, and M. Arai for valuable discussions and technical advice, T. Matta for statistical analysis, I. Smith for editing the manuscript, and M. Tano for secretarial assistance. lt-NES® is a registered trademark of LIFE & BRAIN GmbH, Bonn, Germany.

Disclosure of Potential Conflicts of Interest

The authors indicate no potential conflicts of interest.

References

1 Ditunno JF, Formal CS. Chronic spinal cord injury. N Engl J Med 1994;330:550–556.
2 Ogawa Y, Sawamoto K, Miyata T et al. Transplantation of in vitro-expanded fetal neural progenitor cells results in neurogenesis and functional recovery after spinal cord contusion injury in adult rats. J Neurosci Res 2002;69:925–933.
3 Iwanami A, Kaneko S, Nakamura M et al. Transplantation of human neural stem cells for spinal cord injury in primates. J Neurosci Res 2005;80:182–190.
4 Cummings BJ, Uchida N, Tamaki SJ et al. Human neural stem cells differentiate and promote locomotor recovery in spinal cord-injured mice. Proc Natl Acad Sci USA 2005;102:14069–14074.
5 Keirstead HS, Nistor G, Bernal G et al. Human embryonic stem cell-derived oligodendrocyte progenitor cell transplants remyelinate and restore locomotion after spinal cord injury. J Neurosci 2005;25:4694–4705.
6 Sharp J, Frame J, Siegenthaler M et al. Human embryonic stem cell-derived oligodendrocyte progenitor cell transplants improve recovery after cervical spinal cord injury. Stem Cells 2010;28:152–163.
7 Takahashi K, Yamanaka S. Induction of pluripotent stem cells from mouse embryonic and adult fibroblast cultures by defined factors. Cell 2006;126:663–676.
8 Takahashi K, Tanabe K, Ohnuki M et al. Induction of pluripotent stem cells from adult human fibroblasts by defined factors. Cell 2007;131:861–872.
9 Nori S, Okada Y, Yasuda A et al. Grafted human-induced pluripotent stem-cell-derived neurospheres promote motor functional recovery after spinal cord injury in mice. Proc Natl Acad Sci USA 2011;108:16825–16830.
10 Koch P, Opitz T, Steinbeck JA et al. A rosette-type, self-renewing human ES cell-derived neural stem cell with potential for in vitro instruction and synaptic integration. Proc Natl Acad Sci USA 2009;106:3225–3230.
11 Falk A, Koch P, Kesavan J et al. Capture of neuroepithelial-like stem cells from pluripotent stem cells provides a versatile system for in vitro production of human neurons. PLoS One 2012;7:e29597.
12 Kim HT, Kim IS, Lee IS et al. Human neurospheres derived from the fetal central nervous system are regionally and temporally specified but are not committed. Exp Neurol 2006;199:222–235.
13 Conti L, Pollard SM, Gorba T et al. Niche-independent symmetrical self-renewal of a mammalian tissue stem cell. PLoS Biol 2005;3:e283.
14 Pollard SM, Conti L, Sun Y et al. Adherent neural stem (NS) cells from fetal and adult forebrain. Cereb Cortex 2006;16 Suppl 1:i112–i120.
15 Abematsu M, Tsujimura K, Yamano M et al. Neurons derived from transplanted neural stem cells restore disrupted neuronal circuitry in a mouse model of spinal cord injury. J Clin Invest 2010;120:3255–3266.
16 Sun Y, Pollard S, Conti L et al. Long-term tripotent differentiation capacity of human neural stem (NS) cells in adherent culture. Mol Cell Neurosci 2008;38:245–258.
17 Miyoshi H, Blömer U, Takahashi M et al. Development of a self-inactivating lentivirus vector. J Virol 1998;72:8150–8157.
18 Okada S, Ishii K, Yamane J et al. In vivo imaging of engrafted neural stem cells: Its application in evaluating the optimal timing of transplantation for spinal cord injury. FASEB J 2005;19:1839–1841.
19 Basso DM, Fisher LC, Anderson AJ et al. Basso Mouse Scale for locomotion detects differences in recovery after spinal cord injury in five common mouse strains. J Neurotrauma 2006;23:635–659.
20 Setoguchi T, Nakashima K, Takizawa T et al. Treatment of spinal cord injury by transplantation of fetal neural precursor cells engineered to express BMP inhibitor. Exp Neurol 2004;189:33–44.
21 Hata K, Fujitani M, Yasuda Y et al. RGMa inhibition promotes axonal growth and recovery after spinal cord injury. J Cell Biol 2006;173:47–58.
22 Kaneko S, Iwanami A, Nakamura M et al. A selective Sema3A inhibitor enhances regenerative responses and functional recovery of the injured spinal cord. Nat Med 2006;12:1380–1389.
23 Pronichev IV, Lenkov DN. Functional mapping of the motor cortex of the white mouse by a microstimulation method. Neurosci Behav Physiol 1998;28:80–85.
24 Yoshihara Y, Mizuno T, Nakahira M et al. A genetic approach to visualization of multisynaptic neural pathways using plant lectin transgene. Neuron 1999;22:33–41.
25 Kinoshita N, Mizuno T, Yoshihara Y. Adenovirus-mediated WGA gene delivery for transsynaptic labeling of mouse olfactory pathways. Chem Senses 2002;27:215–223.
26 Furukawa N, Saito M, Hakoshima T et al. A diphtheria toxin receptor deficient in epidermal growth factor-like biological activity. J Biochem 2006;140:831–841.
27 Saito M, Iwawaki T, Taya C et al. Diphtheria toxin receptor-mediated conditional and targeted cell ablation in transgenic mice. Nat Biotechnol 2001;19:746–750.
28 Luchetti S, Beck KD, Galvan MD et al. Comparison of immunopathology and locomotor recovery in C57BL/6, BUB/BnJ, and NOD-SCID mice after contusion spinal cord injury. J Neurotrauma 2010;27:411–421.
29 Yan J, Welsh AM, Bora SH et al. Differentiation and tropic/trophic effects of exogenous neural precursors in the adult spinal cord. J Comp Neurol 2004;480:101–114.
30 Nothias JM, Mitsui T, Shumsky JS et al. Combined effects of neurotrophin secreting transplants, exercise, and serotonergic drug challenge improve function in spinal rats. Neurorehabil Neural Repair 2005;19:296–312.
31 Kim D, Murray M, Simansky KJ. The serotonergic 5-HT(2C) agonist *m*-chlorophenylpiperazine increases weight-supported locomotion without development of tolerance in rats with spinal transections. Exp Neurol 2001;169:496–500.

32 Courtine G, Song B, Roy RR et al. Recovery of supraspinal control of stepping via indirect propriospinal relay connections after spinal cord injury. Nat Med 2008;14:69–74.

33 Hooshmand MJ, Sontag CJ, Uchida N et al. Analysis of host-mediated repair mechanisms after human CNS-stem cell transplantation for spinal cord injury: Correlation of engraftment with recovery. PLoS One 2009;4:e5871.

34 Yan J, Xu L, Welsh AM et al. Extensive neuronal differentiation of human neural stem cell grafts in adult rat spinal cord. PLoS Med 2007;4:e39.

35 Nakamura M, Houghtling RA, MacArthur L et al. Differences in cytokine gene expression profile between acute and secondary injury in adult rat spinal cord. Exp Neurol 2003;184:313–325.

36 Bareyre FM, Schwab ME. Inflammation, degeneration and regeneration in the injured spinal cord: insights from DNA microarrays. Trends Neurosci 2003;26:555–563.

37 Lu P, Tuszynski MH. Growth factors and combinatorial therapies for CNS regeneration. Exp Neurol 2008;209:313–320.

38 Okita K, Nakagawa M, Hyenjong H et al. Generation of mouse induced pluripotent stem cells without viral vectors. Science 2008; 322:949–953.

39 Zhou H, Wu S, Joo JY et al. Generation of induced pluripotent stem cells using recombinant proteins. Cell Stem Cell 2009;4:381–384.

40 Kaji K, Norrby K, Paca A et al. Virus-free induction of pluripotency and subsequent excision of reprogramming factors. Nature 2009;458: 771–775.

41 Lindvall O, Kokaia Z. Stem cells in human neurodegenerative disorders–time for clinical translation? J Clin Invest 2010;120:29–40.

42 Cao QL, Howard RM, Dennison JB et al. Differentiation of engrafted neuronal-restricted precursor cells is inhibited in the traumatically injured spinal cord. Exp Neurol 2002;177:349–359.

43 Han SS, Kang DY, Mujtaba T et al. Grafted lineage-restricted precursors differentiate exclusively into neurons in the adult spinal cord. Exp Neurol 2002;177:360–375.

44 Louro J, Pearse DD. Stem and progenitor cell therapies: recent progress for spinal cord injury repair. Neurol Res 2008;30:5–16.

45 Jain KK. Cell therapy for CNS trauma. Mol Biotechnol 2009;42: 367–376.

46 Bareyre FM, Kerschensteiner M, Raineteau O et al. The injured spinal cord spontaneously forms a new intraspinal circuit in adult rats. Nat Neurosci 2004;7:269–277.

47 Shumsky JS, Tobias CA, Tumolo M et al. Delayed transplantation of fibroblasts genetically modified to secrete BDNF and NT-3 into a spinal cord injury site is associated with limited recovery of function. Exp Neurol 2003;184:114–130.

48 Tobias CA, Shumsky JS, Shibata M et al. Delayed grafting of BDNF and NT-3 producing fibroblasts into the injured spinal cord stimulates sprouting, partially rescues axotomized red nucleus neurons from loss and atrophy, and provides limited regeneration. Exp Neurol 2003;184: 97–113.

49 Erceg S, Ronaghi M, Oria M et al. Transplanted oligodendrocytes and motoneuron progenitors generated from human embryonic stem cells promote locomotor recovery after spinal cord transection. Stem Cells 2010;28:1541–1549.

50 Siegenthaler MM, Tu MK, Keirstead HS. The extent of myelin pathology differs following contusion and transection spinal cord injury. J Neurotrauma 2007;24:1631–1646.

51 Miura K, Okada Y, Aoi T et al. Variation in the safety of induced pluripotent stem cell lines. Nat Biotechnol 2009;27:743–745.

52 Tsuji O, Miura K, Okada Y et al. Therapeutic potential of appropriately evaluated safe-induced pluripotent stem cells for spinal cord injury. Proc Natl Acad Sci USA 2010;107:12704–12709.

53 Jensen JB, Parmar M. Strengths and limitations of the neurosphere culture system. Mol Neurobiol 2006;34:153–161.

See www.StemCells.com for supporting information available online.

1C3-3

現実およびバーチャルリアリティ空間におけるマウスの肢刺激を手掛かりとした弁別課題の確立

本間千尋[1)]、山田一之[1)]、鴨志田敦史[1,2)]、茂泉俊次郎[1,3)]、鮫島正大[1,3)]、織田充[1)]、山川宏[1)]、○村山正宜[1)]

(1) 理研 BSI 行動神経生理、2) 日本ナショナルインスツルメンツ、3) ソリッドレイ研究所)

New experimental systems for a tactile discrimination task in real and virtual world

Chihiro Homma[1)], Kazuyuki Yamada[1)], Atsushi Kamoshida[1,2)], Shunjiro Moizumi[1,3)], Masahiro Samejima[1,3)], Mitsuru Oda[1)], Hiroshi Yamakawa[1)], * Masanori Murayama[1)]

(1)Lab for Behav Neurophysiol, BSI, RIKEN, 2) National Instruments Japan Corporation, 3) Solidray Corporation)

Abstract— Cutaneous sensations are thought to be represented in primary somatosensory cortex (S1) as a result of neural activity, which can then be used for higher brain functions such as decision-making, attention, and memory. In a previous study we showed that the intensity of limb stimulation in rodents is coded by the dendritic activity of layer 5 pyramidal neurons in S1. This implies that somatosensation of tactile stimuli can also be used as a primary mode of input that is sent to higher brain areas. To further test this hypothesis, we developed a new experimental system in which mice discriminated texture in a modified Y-maze, from these results, we are now applying this task in virtual world situations.

Key Words: somatosensation, discrimination, Y-maze

1 はじめに

体性感覚は空間や環境を認知するにあたり大きな役割を担っている。特にげっ歯類が環境を認知する際は体性感覚情報に強く依存しており、この特性を利用した学習や意思決定等を含んだ高次脳機能の神経科学的な解明を試みた研究が昨今多く報告されている[1,2]。しかしいまだその神経メカニズムは未知の部分が多い。そこで本研究では、マウス自由行動下にて体性感覚情報が高次脳領域へ到達するまでの神経回路を解明することを目的として、体性感覚刺激を手がかりとした弁別課題の実施可能な自動化 Y 迷路装置を作成した。本装置はすべて自動化されており、電気生理学などの他の技術的手法を合わせて使用しやすくまた動物を用いた学習訓練に特有の実験者への負担を軽減することもできる。

一方、脳機能の神経科学的アプローチの一つの手法として、脳のイメージング法があるが、二光子顕微鏡などの大型装置を使用したイメージングを行うためには頭部固定化で実験を行う必要があり、そのため VR システムの搭載が便利であり昨今広く使用されている[3,4]。我々は現実空間における Y 迷路課題の訓練結果に基づいてバーチャルリアリティ (VR) 空間における Y 迷路課題の確立を試みており、ここにその進捗を報告する。

2 現実空間における Y 迷路課題

2.1 装置および実験方法

本装置は通常の Y 迷路とは異なり終点と始点が連結した形状をしている。また試行開始および終了時に開閉する扉と触覚呈示部分、加えて報酬取得部分がすべて自動化されている。さらに自動化部分はすべてソフトウェア (LabVIEW 2011 ver.11, National Instruments) で制御されており、学習が成立するまでの一連の訓練を自動で行うことができ、手技の統一および時間や手間の効率化をはかることができる (Fig. 1)。

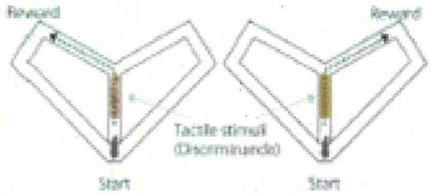

Fig.1: Automated Y-maze

マウスは 6 週齢以降の C57BL/6J (日本 SLC) 系統を用いた。訓練は床に設置された触覚刺激 (紙やすり #40 または厚紙) 通過後、正解方向を選択した場合は報酬個所で報酬が得られ、不正解方向を選択した場合は得ることができない、継時弁別訓練法を用いた。

2.2 結果

訓練は各マウスで 30 試行 1 セッションを 1 日に 1 回行った。訓練が重なるにつれマウスは徐々に装置の特性をつかみ、報酬獲得後すぐに開始部分に戻るようになる (Fig. 2)。訓練は初めに一種類の触覚刺激と

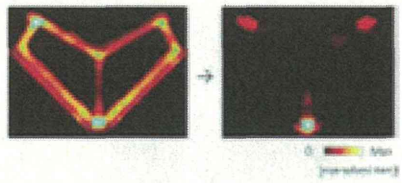

Fig. 2: Representative data sample of time spent duration of mouse's location during the training

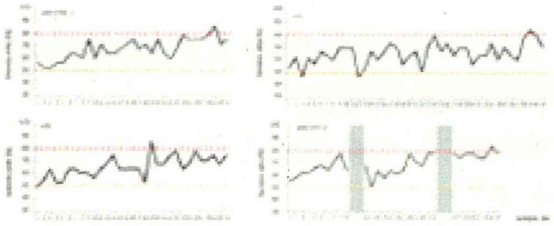

Fig. 3: Learning curve of discrimination training
Red dashed line; 80% of success rate, Yellow dashed line; chance level, Gray zone; rest period of training

それに対応する片一方向の連合学習を形成させ、両刺激の学習獲得が確認できた後、準無作為に刺激を呈示しさらに訓練を続けた。その結果、現在のところ 5 匹のマウスで約 80%の正解率を示した。Fig. 3 に4個体の正解率の推移を示した。

3 VR 空間における Y 迷路課題

3.1 装置および実験方法

開発した VR システムはマウスの水平視野を 270 度覆う円柱様型のスクリーンと一軸式回転型の回し車、報酬供給装置から構成される。VR 環境はソフトウェア（OmegaSpace ver.3.2, Solidray. Co.）を使用して作成した。また回し車には制御可能な触覚呈示部分が存在し、VR 環境と回し車および触覚呈示部分の動作、報酬供給装置はすべてソフトウェア (LabVIEW 2011 ver.11)で制御可能とし、本装置も一連の訓練を自動で行うことができる（Fig. 4）。マウスの進行方向はマウスの頭部と体の重心の角度より決定した。

使用したマウスの条件は前述と同様であり、訓練前に頭部固定化で行うためチタン製ヘッドプレートを接着した。訓練は初めに VR 空間に馴致するため直線走路課題を行い、一定距離走行することで報酬を得ることのできる道具的条件付けを行った。滑滑な走行を確認した後、VR-Y 迷路課題に移行した（Fig. 5）。

3.2 結果

訓練は各マウスで 30 試行 1 セッションを 1 日に 1 回行った。直線走路課題開始時は進行方向を決定する角度情報の分散が大きく、訓練が進むにつれ分散が小さくなり、1 セッションあたりの平均回転速度も大

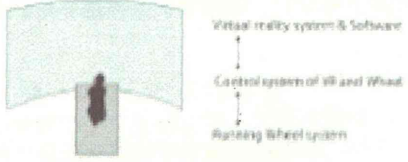

Fig. 4: VR system

Fig. 5: Y-maze in VR world
Picture before the branch point

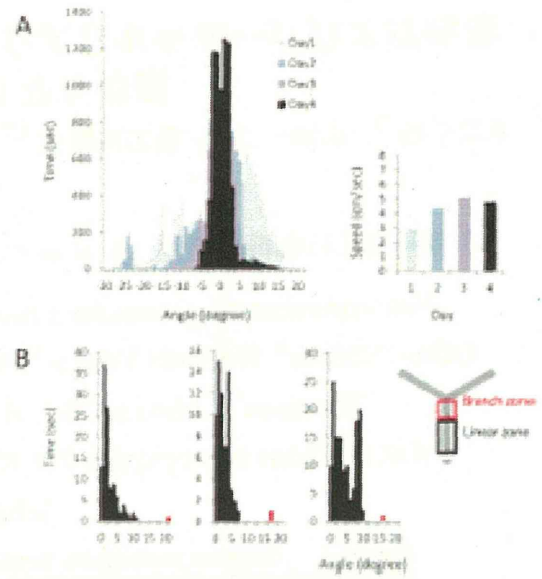

Fig. 6: Representative data sample of accustomising to virtual tracks. B: Each graph represents angle (absolute value) in a trial. Black bar; Range of angle at linear track in Y-maze, Red bar; Maximum angle at branch zone

きくなった（Fig. 6A）。開始時は VR 空間および回し車上の走行に馴致が見られないが、訓練が進むにつれ、いずれにも馴致できたことが示唆される。

VR-Y 迷路課題では Y 迷路分岐部分通過後報酬を与える行動の形成を行ったが、呈示された分岐部分に合わせて体の角度を大きくし左右方向に進もうとするような行動が確認された（Fig. 6B）。

4 まとめ

我々は自動化 Y 迷路を作成し訓練を行うことで、マウスを用いた触覚弁別課題を確立することできた。さらに、その課題を VR 空間内で行えるシステムを構築し、訓練後マウスが VR 空間に準じて動きを変えることが示唆される結果を確認できた。今後は自動化触覚刺激を呈示し弁別課題を試みる予定である。また本両システムを使用し、光遺伝学的手法や電気生理学的手法を用いた脳機能解明へのアプローチを目指し現在準備を進めている。

参考文献

1) Petreanu L, Gutnisky DA, Huber D, Xu NL, O'Connor DH, Tian L, Looger L, Svoboda K.: Activity in motor-sensory projections reveals distributed coding in somatosensation., Nature. 489(7415), 299/303 (2012)
2) Maricich S M, Morrison K M, Mathes E L, Brewer B M.: Rodents rely on Merkel cells for texture discrimination tasks., J Neurosci. 32(10), 3296/3300 (2012)
3) Harvey CD, Collman F, Dombeck DA, Tank DW.: Intracellular dynamics of hippocampal place cells during virtual navigation., Nature. 461(7266), 941/946 (2009)
4) Youngstrom IA, Strowbridge BW.: Visual landmarks facilitate rodent spatial navigation in virtual reality environments., Learn Mem., 19(3), 84/90 (2012)